Radiolytic and Hydrolytic Degradation of the Hydrophilic Diglycolamides

Andreas Wilden[a,*], Bruce J. Mincher[b], Stephen P. Mezyk[c], Liam Twight[c], Kristyn M. Rosciolo-Johnson[b], Christopher A. Zarzana[b], Mary E. Case[b], Michelle Hupert[d], Andrea Stärk[d], Giuseppe Modolo[a]

a. Forschungszentrum Jülich GmbH, Institut für Energie- und Klimaforschung – Nukleare Entsorgung und Reaktorsicherheit (IEK-6), Jülich, Germany; *a.wilden@fz-juelich.de
b. Idaho National Laboratory, Idaho Falls, ID, 83415, USA
c. Department of Chemistry and Biochemistry, California State University at Long Beach, Long Beach, CA, 90840, USA
d. Forschungszentrum Jülich GmbH, Zentralinstitut für Engineering, Elektronik und Analytik (ZEA-3), Jülich, Germany

ORCID

Andreas Wilden:	0000-0001-5681-3009
Giuseppe Modolo:	0000-0001-6490-5595
Bruce J. Mincher:	0000-0003-3108-2590
Stephen P. Mezyk:	0000-0001-7838-1999
Christopher A. Zarzana	0000-0001-9617-7123
Michelle Hupert	0000-0002-1179-573X
Andrea Stärk	0000-0002-2922-7167

KEYWORDS

Hydrolysis; Radiolysis; Pulse radiolysis; diglycolamides; TEDGA; Radical reaction

ABSTRACT

The stability of different hydrophilic diglycolamides against acid degradation and radiolysis was studied. Tetraethyldiglycolamide (TEDGA) was found to undergo degradation in nitric acid at high reaction rates at elevated temperatures with a maximum of a ~8% decrease per hour at 65°C in 4 mol L^{-1} HNO_3. The radiolysis was studied for tetramethyldiglycolamide (TMDGA), TEDGA, methyl-tetraethyldiglycolamide (Me-TEDGA), and dimethyl-tetraethyldiglycolamide (Me_2-TEDGA). The degradation rates decreased with increasing molecular weight, following the trend TMDGA > TEDGA > Me-TEDGA ≥ Me_2-TEDGA. Degradation products were identified by mass spectrometric techniques and were found to be comparable to those previously reported for the radiolysis of lipophilic diglycolamides in dodecane. Significant insight into the degradation mechanism in water was gained using pulse radiolysis experiments. The $^{\bullet}OH$ radical was identified as the most important reactive species and predominant mechanism of radical reaction is one of electron transfer rather than H-atom abstraction.

INTRODUCTION

The diglycolamide (DGA) family of ligands is currently being studied for use in processes to separate actinides from used nuclear fuel. The influence of DGA structure on separation factors for actinides from the lanthanides is of particular interest. This has resulted in the study of many DGA derivatives. When the DGA N-alkyl substituents were varied, it was found that short chain compounds have decreased solubility in the alkane diluents typical of fuel cycle solvent extraction organic phases. For example, the intermediate chain length tetrabutyldiglycolamide (TBDGA) has been used for americium and lanthanide extraction in 1-octanol diluent, [1] while the shorter chain tetraethyldiglycolamide (TEDGA) and tetramethyldiglycolamide (TMDGA) are water soluble, [2] and have been used as aqueous stripping and hold back agents. Tetraethyldiglycolamide has been used to strip lanthanides from the ALSEP (Actinide Lanthanide Separation) solvent to regenerate that solvent for recycle. [3] Similarly, the EXtraction of Americium (EXAm) process uses TEDGA to enable a separation of the lanthanides and curium from americium. [4] Very recently, Lange et al. [5] reported a separation of americium from curium using a lipophilic soft donor extractant and water-soluble TEDGA, in which a separation factor $SF_{Am/Cm} = 4.9$ for tracer experiments was obtained. A lower $SF_{Am/Cm} = 2.4$ was obtained in experiments using a PUREX raffinate simulant; however, with $D_{Am} > 1$ and $D_{Cm} < 1$, excellent separation from the lanthanides was observed. Thus, interest in hydrophilic DGAs is current, and the chemistry of the DGAs with special emphasis on actinide separations has been reviewed. [6]

An understanding of the influence of radiation on separation ligands is critical to the development and implementation of robust fuel cycle processes. Additionally, the influence of acid degradation is important, especially for water-soluble ligands. For the lipophilic DGAs, several reports have recently appeared providing radiolytic degradation rates under various solution conditions including with and without contact with acidic aqueous phases, and identification of radiolysis products using state-of-the-art analytical techniques. These have included studies of the radiation chemistry of tetraoctyldiglycolamide (TODGA) and tetra(2-ethylhexyl)diglycolamide (TEHDGA), [7] didodecyldioctyldiglycolamide (D^3DODGA), [8] and methyl-tetraoctyldiglycolamide (Me-TODGA) and dimethyl-tetraoctyldiglycolamide (Me_2-TODGA). [9] Unlike many other fuel cycle ligands, all the lipophilic DGAs in dodecane diluent were degraded by γ-irradiation with about the same dose constant (kGy^{-1}), and that rate did not vary significantly in the presence or absence of contact with aqueous phases of varying acidity. Common products of irradiation were trialkyldiglycolamides produced by loss of an alkane group from one of the N–atoms, production of carboxylic acids following C–N bond rupture with loss of the amine group, and acetamides and glycolamides resulting from rupture of the central ether linkage. Radical cations produced in the irradiated alkane

diluent have been implicated as the reactive species that initiate lipophilic DGA degradation. [10, 11]

We are not aware of previous work that investigates the radiation chemistry of DGAs in aqueous solution. The aqueous matrix gives rise to a completely different set of reactive species than does the organic phase when irradiated and therefore it was deemed interesting to measure the rates of degradation and identify the products of the radiolysis of hydrophilic DGAs and compare them to previous organic-phase work. This was expected to provide mechanistic insights, as well as to generate data of use to the design of fuel cycle separations processes. Here, the radiolysis of TMDGA, TEDGA, Me-TEDGA, and Me_2-TEDGA were examined. Data with respect to the acid degradation of TEDGA are also presented. The structures of the compounds used in this study are shown in Figure 1.

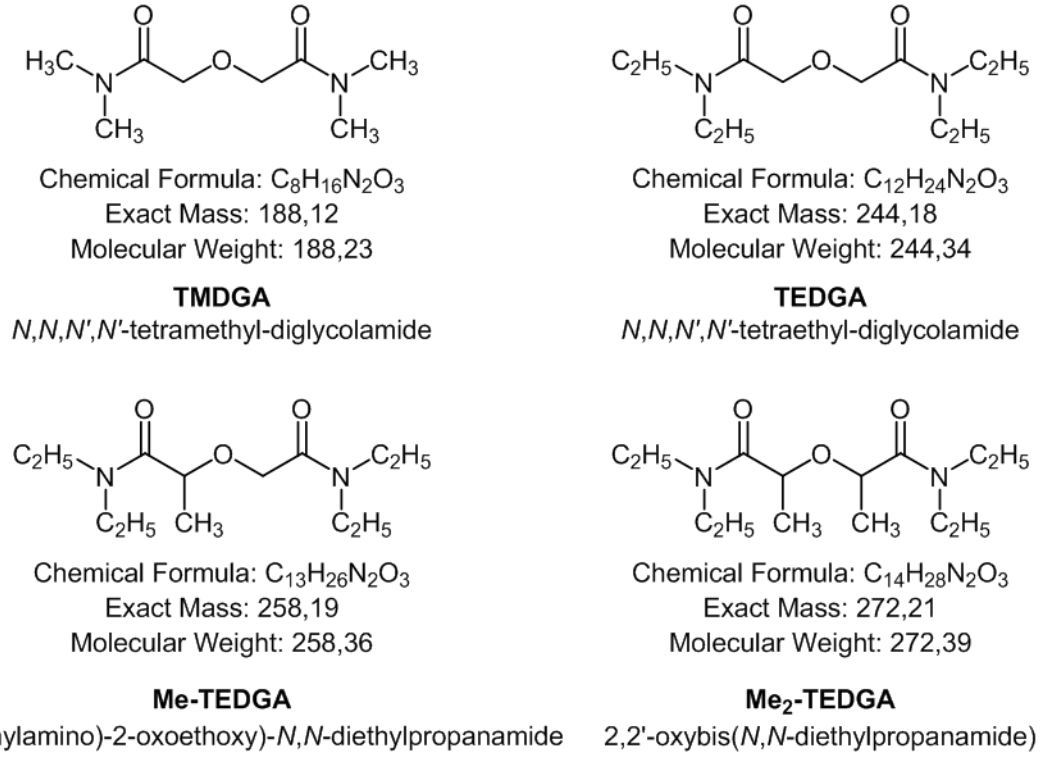

Figure 1. Chemical structures of the hydrophilic DGAs used in this study.

EXPERIMENTAL

Diglycolamides

The DGAs TMDGA, TEDGA, Me-TEDGA, and Me_2-TEDGA were supplied by Technocomm Ltd. (Wellbrae, Falkland, Scotland) and were used as received. The diluent was nanopure water demineralized to a resistivity > 10 MOhm cm prior to use.

Acid degradation and analysis

Solutions of 0.05 mol L^{-1} TEDGA in 0.5 mol L^{-1} and 4.0 mol L^{-1} HNO_3 were held at temperatures of 25, 35, 45, 55, and 65°C for varying durations after which they were sampled and analyzed by ultra-high performance liquid chromatography – electrospray ionization mass spectrometry (UHLP-ESI-MS) at Idaho National Laboratory (INL). The samples were diluted in 50:50 H_2O:Optima® LC/MS Acetonitrile (Fisher Scientific) and then analyzed using a Dionex (Sunnyvale) UHPLC with an Ultimate 3000 RS pump, 3000 RS autosampler, 3000 RS column compartment and a 3000 RS diode array detector, coupled to a Bruker (Billerica) microTOFQ-II electrospray ionization quadrupole time-of-flight mass spectrometer with Hystar 3.2 software.

The chromatographic separation was achieved using 5 µL injections on a Kinetex 1.3 µm C18 50 mm × 2.1 mm column (Phenomenex) held at 50°C. The aqueous component was Optima® LC/MS water with 0.1% v/v formic acid (Fisher Scientific), and the organic component was Optima® LC/MS acetonitrile with 0.1% v/v formic acid (Fisher Scientific). An isocratic mobile phase profile was used with a flow rate of 200 µL min^{-1} and 60% aqueous mobile phase with a 3 minute run time. The mass spectrometer conditions were: capillary: 4.5 kV, positive mode; temp.: 220°C; nebulizer gas and dry gas were both N_2, nebulizer pressure: 0.4 bar; dry gas flow rate: 9 L min^{-1}. The mass spectrometer was operated using standard Bruker tuning parameters, specifically "tune low". Each sample was injected 5 times.

For comparison, 0.05 mol L^{-1} TEDGA was also held at 65°C in 5 and 8 mol L^{-1} HCl. These samples were analyzed by the same technique.

γ-Irradiation

Steady state γ-irradiations were performed at INL using a ^{60}Co-Nordion Gammacell 220, at a dose rate of 3.8 kGy h^{-1}, as initially measured using standard Fricke procedures, and then subsequently corrected for decay. The DGAs were irradiated as initially 0.05 mol L^{-1} solutions in nanopure water to target absorbed doses of 0, 25, 50, 75, 100, 125 and 150 kGy, in sealed containers. The temperature in the sample chamber during irradiation is 23 ± 2°C. Neutral water was chosen to allow for the study of radiolysis in the absence of the confounding acid degradation effects expected in acidic solution. After irradiation the samples were delivered to Forschungszentrum Jülich (FZJ) for analysis.

Analysis of DGA concentration in irradiated samples

Irradiated samples were analyzed at FZJ by high performance liquid chromatography – electrospray ionization mass spectrometry/mass spectrometry (HPLC-ESI-MS/MS). The chromatographic separations varied slightly with the DGA analyte. All samples were diluted 1:500,000 and measured in triplicate.

For TMDGA, a Phenomenex Kinetex-HILIC (100 × 4.6 mm; 2.6 µm particle size) column was used with a gradient of acetonitrile + 0.1% formic acid (A) in 10 mmol L^{-1} ammonium acetate

buffer in H_2O at pH 5.5 (B), 40°C and a flow-rate of 900 µL min^{-1}. The gradient is described in Table SI 1. The calibration was done using the unirradiated TMDGA samples by dilution. The linearity was found to be good in the region from 5 nmol L^{-1} to 500 nmol L^{-1} with R^2 = 0.9998. The variation coefficient of a 100 nmol L^{-1} standard of TMDGA was 2.5%.

For TEDGA and Me-TEDGA, a Thermo Phenyl-X (100 × 4.6 mm; 2.6 µm particle size) column was used with a gradient of acetonitrile + 0.1% formic acid (A) in 0.1% formic acid in H_2O (B) at 35°C and a flow-rate of 800 µL min^{-1}. The gradient is described in Table SI 2. The calibration was done using the unirradiated TEDGA and Me-TEDGA samples by dilution. The linearity was found to be good in the region from 10 nmol L^{-1} to 500 nmol L^{-1} with R^2 = 0.9955, and 0.9991, respectively. The variation coefficients of a 100 nmol L^{-1} standard were 7.4% and 6.2%, respectively.

For Me_2-TEDGA, a Phenomenex Luna Omega C18 Polar (100 × 4.6 mm; 2.6 µm particle size) column was used with a gradient of acetonitrile + 0.1% formic acid (A) in 0.1% formic acid in H_2O (B) at 35°C and a flow-rate of 800 µL min^{-1}. The gradient is described in Table SI 3. The calibration was done using the unirradiated Me_2-TEDGA samples by dilution. The linearity was found to be good in the region from 1 nmol L^{-1} to 500 nmol L^{-1} with R^2 = 0.9997. The variation coefficient of a 100 nmol L^{-1} standard of Me_2-TEDGA was 8.2%.

HPLC-ESI-MS/MS for quantification was performed with a Qtrap6500 instrument (ABSciex, Darmstadt) coupled with an Agilent 1260 HPLC system consisted of a binary pump system, an autosampler and a thermostated column compartment. The MS parameters used for all methods were optimized by performing a Flow Injection Analysis (FIA) with standards and led to the following settings for all analysis: curtain gas (N_2) 40 arbitrary units (a.u.), temperature of the source 350°C, nebulizer gas (N_2) 40 a.u. and heater gas (N_2) 80 a.u. Quantification after HPLC was performed using ESI-MS/MS detection in the multiple reaction-monitoring (MRM) mode in positive ionization mode. MRM transitions involving precursor ions $(M+H)^+$ and the two most abundant product ions were used for quantification of all analytes as shown in Table SI 4. All LC-MS/MS data acquisition and processing was carried out using the Software Analyst 1.6.1 (AB Sciex, Darmstadt). Quantification was performed with the Software Multiquant (AB Sciex, Darmstadt).

Degradation product identification in irradiated samples

Product analysis was performed at FZJ using a hybrid linear ion trap FTICR (Fourier-Transform Ion Cyclotron Resonance) mass spectrometer LTQFT (Linear Tandem Quadrupole Fourier Transform) Ultra™ (Thermo Fisher Scientific, Bremen) coupled with an Agilent 1200 HPLC system consisted of a binary pump system, an autosampler, a thermostated column compartment and a Diode-Array detector (Agilent, Waldbronn). The mass spectrometer was first tuned and calibrated in the positive mode following the standard optimization procedure for all voltages and settings: Source Type: ESI, Ion Spray Voltage: 3.8 kV, Capillary Voltage: 37.00 V, Tube Lens; 130.00 V, Capillary Temp: 275.00°C, Sheath Gas Flow: 60.00. Mass spectra were

recorded in full scan from 50 to 500 Da (TMDGA) or 100 to 1000 Da (TEDGA, Me-TEDGA, and Me_2-TEDGA) with a resolution of 100,000 at *m/z* 400. All data were processed using the Xcalibur software version 2.0.

Pulse radiolysis

Pulse radiolysis experiments were performed using the LINAC system at the University of Notre Dame Radiation Laboratory, using previously described techniques. [15] Although $^{\bullet}OH$ radical kinetics are typically measured using thiocyanate competition, the direct product of the reaction with hydrophilic DGAs has significant transient absorbance in the UV/Vis region and thus direct measurements were performed at 380 nm and 420 nm for TMDGA and TEDGA, respectively.

RESULTS AND DISCUSSION

Acid degradation

The change in TEDGA concentration versus contact time for TEDGA samples in contact with 0.5 mol L^{-1} HNO_3 and 4.0 mol L^{-1} HNO_3 at 5 different temperatures is shown in Figure 2. The concentration changes may be fit with exponential curves, resulting 1st-order rate constants (*k*). These values are shown for each system in Table 1.

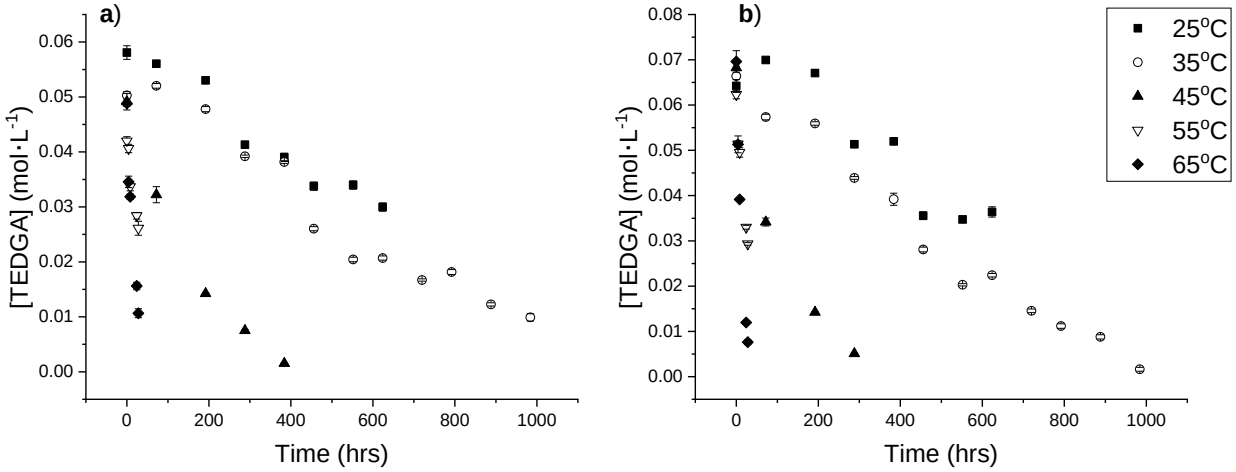

Figure 2. Change in TEDGA concentration versus time, for contact with a) 0.5 mol·L^{-1} and b) 4.0 mol·L^{-1} HNO_3 at various temperatures. Each point is the mean of five measurements and the error bars represent 99% confidence intervals.

Table 1. Measured rate constants (k, h^{-1}) for the degradation of initially 0.05 mol L^{-1} TEDGA across a range of temperatures for HNO_3 and HCl.

T (°C)	0.5 mol L^{-1} HNO_3	4.0 mol L^{-1} HNO_3	5.0 mol L^{-1} HCl	8.0 mol L^{-1} HCl
25	$(1.12 \pm 0.1) \times 10^{-3}$	$(1.22 \pm 0.2) \times 10^{-3}$		
35	$(1.74 \pm 0.1) \times 10^{-3}$	$(2.32 \pm 0.2) \times 10^{-3}$		
45	$(8.54 \pm 0.1) \times 10^{-3}$	$(8.77 \pm 0.5) \times 10^{-3}$		
55	$(1.66 \pm 0.4) \times 10^{-2}$	$(2.54 \pm 0.2) \times 10^{-2}$		
65	$(5.00 \pm 0.6) \times 10^{-2}$	$(7.75 \pm 0.6) \times 10^{-2}$	$(7.0 \pm 0.4) \times 10^{-2}$	$(5.2 \pm 0.2) \times 10^{-2}$

The degradation rate constant for TEDGA increased with both temperature and nitric acid concentration. When these data were used to construct Arrhenius plots the resulting curves were concave rather than linear, indicating sub–Arrhenius behavior with rate constants lower than expected at higher temperatures. This may indicate a change in the degradation mechanism across the temperature range investigated. The highest rate constant measured here was for the loss of TEDGA in 4 mol L^{-1} HNO_3 at 65°C of nearly 8×10^{-2} h^{-1} corresponding to a loss of TEDGA of ~8 % per hour. At 25°C, the loss of TEDGA is only about 1% h^{-1} at the same HNO_3 concentration.

For comparison, the TEDGA degradation rate constants were also obtained for 5 mol L^{-1} and 8 mol L^{-1} HCl at 65°C. These higher HCl concentrations are typical of hydrometallurgical separations for the lanthanides. [12] The degradation rate constant in 5 mol L^{-1} HCl was $(7.0 \pm 0.4) \times 10^{-2}$ h^{-1} at 65°C, similar to the value for 4 mol L^{-1} HNO_3 at that temperature in Table 1. Interestingly, as also shown in Table 1, the rate appears to decrease for higher [HCl], with a value of $(5.2 \pm 0.2) \times 10^{-2}$ h^{-1} in 8 mol L^{-1} HCl at 65°C. This may indicate that degradation rates do not continue to increase with acid concentration at such high HCl concentrations, but that in HNO_3 an oxidation reaction may also become important with increasing [HNO_3]. In any case, at the temperatures of 25–35°C at which a process might operate, the loss of TEDGA is small, even in 4 mol L^{-1} HNO_3. However, non-radiolytic degradation does occur, and since its products may be similar to those of radiolysis, the irradiation experiments in this study were performed in neutral water to minimize confounding effects that could arise during sample transportation or storage time prior to analysis.

Steady State Radiolysis

The radiolytic decrease in all the hydrophilic DGAs examined was exponential with respect to absorbed dose. This is shown in Figure 3 for the different DGAs, and is consistent with the kinetics reported in our previous work with lipophilic DGAs. [7–9] The dose constant d of TEDGA from Figure 3 is 11.1×10^{-3} kGy^{-1} (TEDGA1), which corresponds to a G_o-value of 0.56 μmol J^{-1}. A replicate set of irradiations (TEDGA2) resulted in $d = 9.5 \times 10^{-3}$, and $G_o = 0.48$ μmol J^{-1}, for mean values of $(10.3 \pm 1.13) \times 10^{-3}$ kGy^{-1}, and 0.52 ± 0.06 μmol J^{-1}. This rate of radiolytic degradation is about twice that reported for lipophilic DGAs such as TODGA and TEHDGA, [7] D^3DODGA, [8], and the Me-TODGAs. [9] These values, and those for the other hydrophilic

DGAs are shown in Table 2. It can be seen in Table 2 that the degradation rates for the hydrophilic DGAs decreased with the increasing molecular weight, following the trend TMDGA > TEDGA > Me-TEDGA ≥ Me_2-TEDGA.

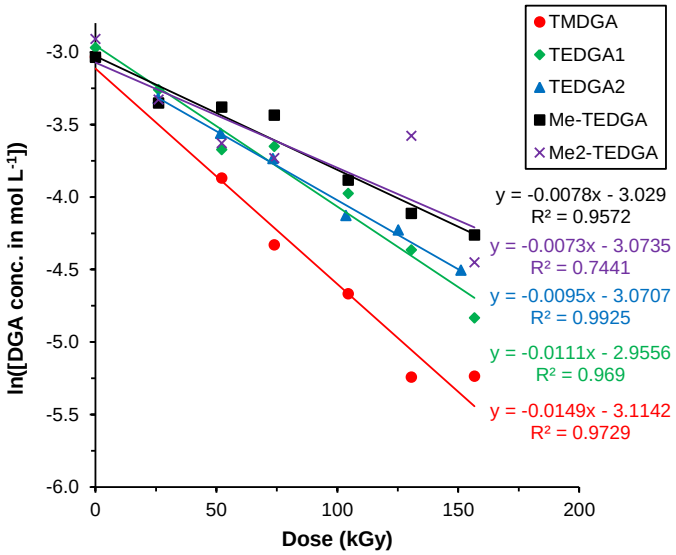

Figure 3. Plot of natural logarithms of DGA concentrations in water for initially 0.05 mol L^{-1} DGA, versus absorbed radiation dose.

Table 2. Dose constants for the degradation of hydrophilic diglycolamides

Diglycolamide	Dose constant d (kGy^{-1})	G_0 (μmol J^{-1})
TMDGA	$(14.9 \pm 1.2) \times 10^{-3}$	−0.74 ± 0.06
TEDGA trial 1	$(11.1 \pm 0.9) \times 10^{-3}$	−0.56 ± 0.04
TEDGA trial 2	$(9.5 \pm 0.4) \times 10^{-3}$	−0.49 ± 0.02
Me-TEDGA	$(7.8 \pm 0.7) \times 10^{-3}$	−0.39 ± 0.04
Me_2-TEDGA	$(7.3 \pm 2.1) \times 10^{-3}$	−0.36 ± 0.11

Dose constants have now also been reported for many lipophilic DGAs in dodecane over a range of carbon chain lengths and the degradation rates were similar for samples irradiated under a variety of conditions, including in pure dodecane solution, and when in contact with aqueous phases of varying acidity or in the presence or absence of air sparging. [7–9] Their dose constants are lower than the values reported for the hydrophilic DGAs in Table 2.

Radiolysis Product Identification

Irradiated samples of the different hydrophilic diglycolamides were analyzed by HPLC-MS at high-resolution. The high resolution enabled an identification of the radiolysis products by their molecular weights (more precisely the *m/z* ratios) and the corresponding chemical formulae. Furthermore, the intensity of the degradation products was followed as a function of the absorbed dose by measuring the area of the corresponding peaks in the chromatograms when only the derived *m/z* ratio was monitored. Although this method is not precisely quantitative, as ionization potentials are different for different fragments and also depending on the total ion count, a rough estimate of the change in abundance of a product in the samples can be given. The *m/z* ratios of the protonated degradation product ions were used, although sodiated product ions, adducts with NH_4^+ ions as well as higher complexes (e.g. 1:2 Na:ligand complexes) were also observed.

Analogous products were identified for the radiolysis of all hydrophilic DGAs examined, and they are partly consistent with the products found for the irradiation of lipophilic DGAs. [7–9] Figure 4 shows a schematic representation of possible degradation reactions and the corresponding products.

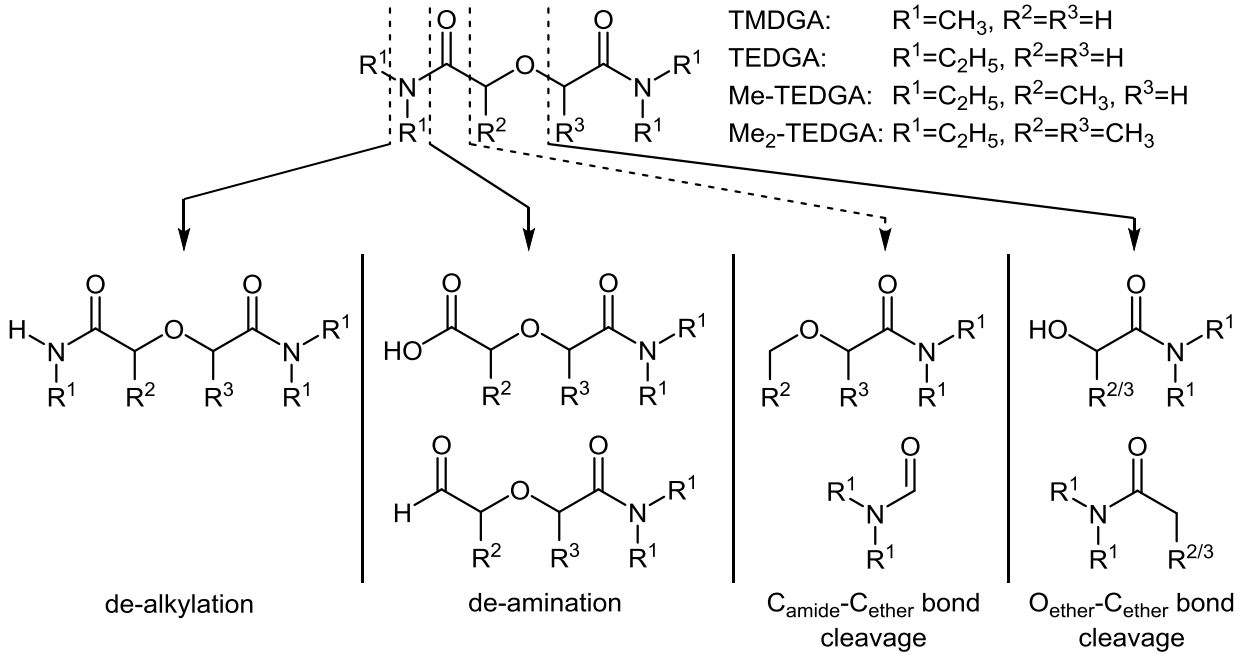

Figure 4. Schematic representation of possible degradation reactions and corresponding products.

De-alkylation products were identified for all hydrophilic DGAs, both for single and double de-alkylation reactions. Single de-alkylations provided products of high signal strength showing a clear increase in abundance with increasing dose (tables SI 6–10). Either no or very little of these

products were found in the unirradiated samples. Products of a double de-alkylation reaction have also been identified and show a similar increase in signal strength with increasing dose, although their abundance is much lower than that of the single de-alkylation reaction (tables SI 6–10). The double de-alkylation degradation fragment can be formed by two de-alkylations of a single amidic nitrogen atom or by two single de-alkylations of two different amidic nitrogen atoms. It's not possible to distinguish between these two paths by the analytical method used here, but the appearance of more than one peak in some chromatograms could be interpreted as both reactions having taken place. Products corresponding to triple or quadruple de-alkylation were not found. Similar de-alkylation reactions have been reported for various lipophilic DGAs, [7–9] CMPO [13] and TBP. [14]

Products of the de-amination reaction (carboxylic acids shown in Figure 4) were found in all irradiated samples. These compounds were also identified in the unirradiated samples and are therefore probably partly left-overs from the synthesis. However, the signal in the irradiated samples was higher and generally increased with absorbed dose. An acidic product such as this could be an important complexing agent that might interfere with separations. The potential de-amination product aldehyde shown in Figure 4 was not detected, perhaps because it hydrolyzes to generate the acid. The other product of the de-amination reaction is a secondary amine. These amines could not be detected, as their masses were lower than low-mass cutoff of the instruments used in this study.

Products of a C_{amide}–C_{ether} bond cleavage could not be identified. Although such products were reported for lipophilic DGAs [7–9] they occurred at low abundance. Thus it is concluded that C–C bond ruptures are relatively rare decomposition mode for the DGAs in both diluents.

The alcohols formed through O_{ether}–C_{ether} bond cleavage were identified in all irradiated samples except the TMDGA samples, and their intensities increased with increasing absorbed dose. That rupture of the ether linkage seems not to occur in the irradiated TMDGA samples suggests that the initiation of ether bond rupture occur in side chains containing secondary carbon atoms. Such an initiation event could be H-atom abstraction, which would be more difficult for tertiary hydrogen atoms of TMDGA than for secondary hydrogen atoms on the longer alkane chains.

The secondary products of O_{ether}–C_{ether} bond cleavage balancing the molecules would give low molecular weight acetamides, but these have not been detected. This may indicate that they undergo hydrolysis or rapid radiolysis upon production, which is different to the lipophilic DGAs irradiated in organic diluent, where these products have been identified. [7–9]

Products corresponding to the hydroxylation of the DGAs were also detected. The two types detected include hydroxylation of the DGA itself, but also hydroxylated de-alkylation products. They were found in all irradiated samples and were absent in the unirradiated samples. Except for TMDGA, the signal intensity of these products increased with increasing dose. This indicates that as additional carbon-centered radical sites are produced with contnued irradiation, as additional hydrogen atoms are abstracted for the alkane chains. In the TMDGA case, hydroxylated products were observed in the first samples but did not continue to grow in with

absorbed dose.. This is also consistent with H-atom abstraction being difficult for the methyl carbons of TMDGA. The initial H-atom abstractions followed by •OH radical addition occur mainly for the two methylene carbon positions on TMDGA. Continued radiolysis does not provide additional opportunity for hydroxylation of this compound.

Interesting products with *m/z* ratios corresponding to the combination of the products of the single de-alkylation and the alcohol radical formed by O_{ether}–C_{ether} bond cleavage were detected. They are attributed to an addition reaction between the radicals initially produced by these bond ruptures, with the corresponding reaction scheme shown in Figure 5. The signal intensities of these recombination products increase with increasing dose and they are not detected in the unirradiated samples. They were found in all irradiated samples except those of TMDGA. This is consistent with the absence of products of O_{ether}–C_{ether} bond cleavage in the irradiated TMDGA samples.

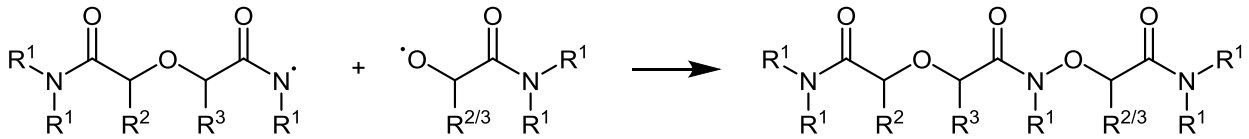

TMDGA: $R^1=CH_3$, $R^2=R^3=H$
TEDGA: $R^1=C_2H_5$, $R^2=R^3=H$
Me-TEDGA: $R^1=C_2H_5$, $R^2=CH_3$, $R^3=H$
Me_2-TEDGA: $R^1=C_2H_5$, $R^2=R^3=CH_3$

Figure 5. Reaction scheme of the combination reaction of the single de-alkylation product radical with the alcohol radical formed by O_{ether}–C_{ether} bond cleavage.

Additionally, *m/z* ratios were observed that could correspond to acetylated molecules of the de-alkylation products. However, it is believed that these products were formed during the analysis, as their retention times were nearly identical to the parent molecules. A tabular overview of the chemical formulae and *m/z* ratios of the protonated species of the found degradation products is given in Table SI 5.

Pulse Radiolysis Measurements

The reaction kinetics of the •OH radical with TMDGA and TEDGA were directly measured by electron pulse radiolysis, through observation of the initially formed intermediate. The obtained bimolecular rate constants were $(3.06 \pm 0.09) \times 10^9$ L mol^{-1} s^{-1} for TMDGA and $(2.91 \pm 0.10) \times 10^9$ L mol^{-1} s^{-1} for TEDGA. Typical data are shown in Figure 6 for the •OH radical as well as the •NO_3 and H-atom reactions with TEDGA. Isolation of individual radicals for study was done by previously established methods. [15] The rate constants for three reactive species measured here for their reactions with TMDGA and TEDGA are shown in Table 3.

Table 3. Bimolecular rate constants (L mol^{-1} s^{-1}) for the reactions of important aqueous transient species with hydrophilic DGAs.

DGA	$^{\bullet}OH$	$^{\bullet}NO_3$	$^{\bullet}H$-atom
TMDGA	$(3.06 \pm 0.09) \times 10^9$	$(3.05 \pm 0.12) \times 10^8$	$(1.22 \pm 0.03) \times 10^8$
TEDGA	$(2.91 \pm 0.10) \times 10^9$	$(6.66 \pm 0.63) \times 10^7$	$(1.60 \pm 0.09) \times 10^8$

Mechanistic Discussion

The reactive species produced in irradiated neutral water and their yields (μmol J^{-1}) are shown in Equation 1. [16]

$$H_2O \text{ -\/\/\/\} \rightarrow [0.28]\ ^{\bullet}OH + [0.27]\ e^-_{aq} + [0.06]\ H^{\bullet} + [0.07]\ H_2O_2 + [0.27]\ H_3O^+ + [0.05]\ H_2 \quad (1)$$

The most reactive species produced in irradiated water is the oxidizing $^{\bullet}OH$ radical, with rate constants approaching the diffusion limit for the reactions measured here. Common reactions of the $^{\bullet}OH$ radical with organic compounds include H-atom abstraction, to produce a carbon-centered radical on the DGA (Equation 2), potentially followed either by radical addition reactions, including with another $^{\bullet}OH$ radical (Equation 3), or by rupture of least stable bonds. The hydroxylated DGAs and hydroxylated de-alkylation products previously discussed are evidence of such H-atom abstraction followed by $^{\bullet}OH$ radical addition reactions as shown in Equation 3.

$$DGA + {}^{\bullet}OH \rightarrow [DGA]^{\bullet} + HOH \quad (2)$$

$$[DGA]^{\bullet} + {}^{\bullet}OH \rightarrow DGA\text{-}OH \quad (3)$$

Another possible reaction pathway for the $^{\bullet}OH$ radical is by electron transfer, shown in Equation 4, in this case producing the DGA radical cation:

$$DGA + {}^{\bullet}OH \rightarrow [DGA]^{\bullet+} + OH^- \quad (4)$$

Based on the products detected by mass spectrometry, formation of these carbon-centered radicals is often followed by rupture of ether C–O bonds or by C–N bond breaks on either side of

the amine N atom. An increase in the number of available target H-atoms would be expected to increase the rate constant for H-atom abstraction by the •OH radical. If H-atom abstraction is a dominant mechanism, this implies that degradation rates (d, kGy^{-1}) across a series of congeners should be faster for higher molecular weights. For example, the rate constant for the reaction of the H-atom, which reacts only by H-atom abstraction, did increase slightly for TEDGA versus TMDGA, as shown in Table 3. However, the measured •OH radical rate constants for TMDGA and TEDGA were the same within experimental uncertainty (Table 3), suggesting a different mechanism is occurring. Further, the aqueous phase d-values were lower for the higher molecular weight DGAs (Table 2), as shown in Fig. 7. This is in contrast to expectations for a dominant H-atom abstraction mechanism, where the presence of a higher number of susceptible hydrogen atoms would be expected to increase the rate constant.

The similar •OH radical reaction rate constants for TMDGA and TEDGA, and the decrease in dose constant with increasing DGA molecular weight are both consistent with an electron transfer mechanism for the •OH radical reaction. Although the rate constants for the electron transfer may be similar across the range of DGA molecular weights, higher molecular weight DGA cations should be more stable, with longer lifetimes providing more opportunity for recombination back-reactions that re-create the DGA molecule. This would account for slower overall degradation rates and thus lower dose constants. The dose constants previously reported for the degradation of the lipophilic DGAs in dodecane solution are also shown in Figure 7, and approximately continue the trend of decreasing degradation rate with increasing molecular weight. Diglycolamide degradation in irradiated dodecane is usually attributed to radical cation electron transfer reactions. [7–9] Produced DGA radical cations then apparently decay to the products found by mass spectrometry. If similar electron transfer reactions with the •OH radical occur in aqueous solution, this would account for the similarity in products detected by mass spectrometry in the disparate diluents.

Alternatively, the •OH radical reaction could be H-atom extraction from the methylene group adjacent to the ether. As shown in Figure 8, this radical could be propagated to the N-terminal ethyl, but not methyl, group. This could facilitate the acid-catalyzed cleavage of the C-O bond, followed by hydrolysis to produce the alcohol.

Radiolytic degradation being initiated in the side-chains of molecules has been observed previously for bistriazinylpyiridine (BTP) and bistriazinylbipyiridine (BTBP) ligands. It was found that annulated BTP and BTBP ligands showed superior stability against radiolytic degradation compared to their linear alkyl chain analogues and this was attributed to the absence of α-CH_2 groups adjacent to the triazinyl moiety. [17–19] Thus, the analogous position in the DGA molecule is a likely site for radical attack, consistent with the mechanism suggested here.

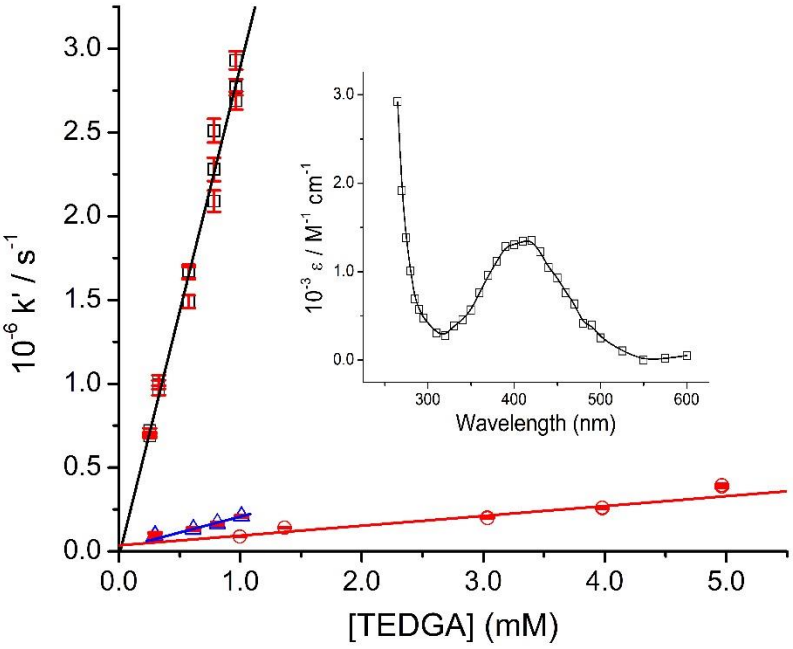

Figure 6. Kinetic data obtained for $^{\bullet}OH$ (□), hydrogen atom (Δ) and $^{\bullet}NO_3$ radical (O) with TEDGA in aqueous solution. Solid lines correspond to weighted linear fits, corresponding to rate constants of $(2.91 \pm 0.10) \times 10^9$, $(6.66 \pm 0.63) \times 10^7$, and $(1.60 \pm 0.09) \times 10^8$ L mol^{-1} s^{-1}, respectively. Inset: Transient absorption spectrum obtained for $^{\bullet}OH$ reaction with TEDGA in N_2O-saturated solution at pH 7.0 and 22°C.

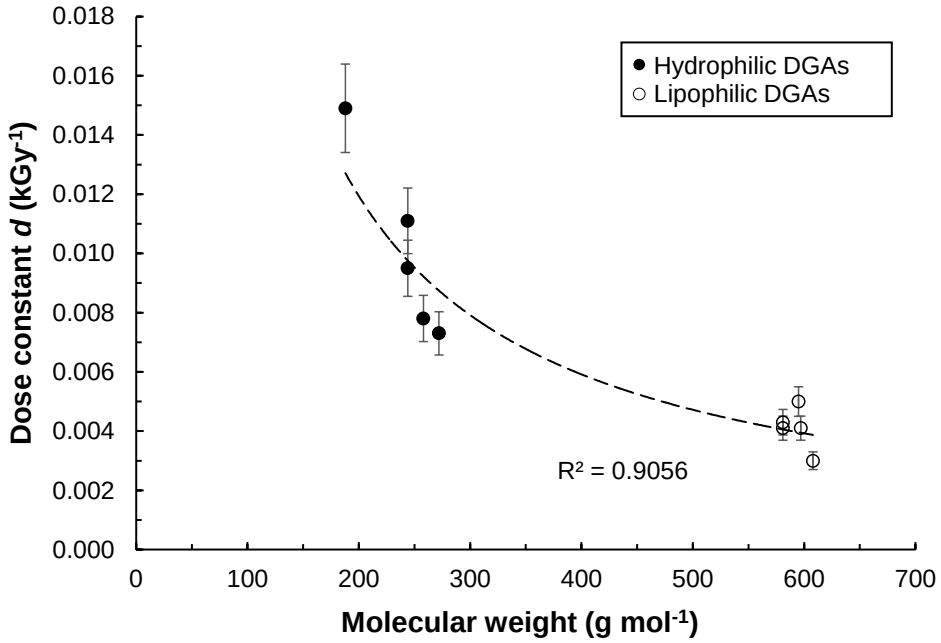

Figure 7. Dose constant (d, kGy^{-1}) for the degradation of DGA versus molecular weight for hydrophilic DGAs (closed circles) and lipophilic DGAs (open circles). Data for lipophilic DGAs is for irradiation of dodecane only with no aqueous phase, from refs [7–9]. Dashed line fit to data is meant to guide the eye only. Error bars shown are ± 10%.

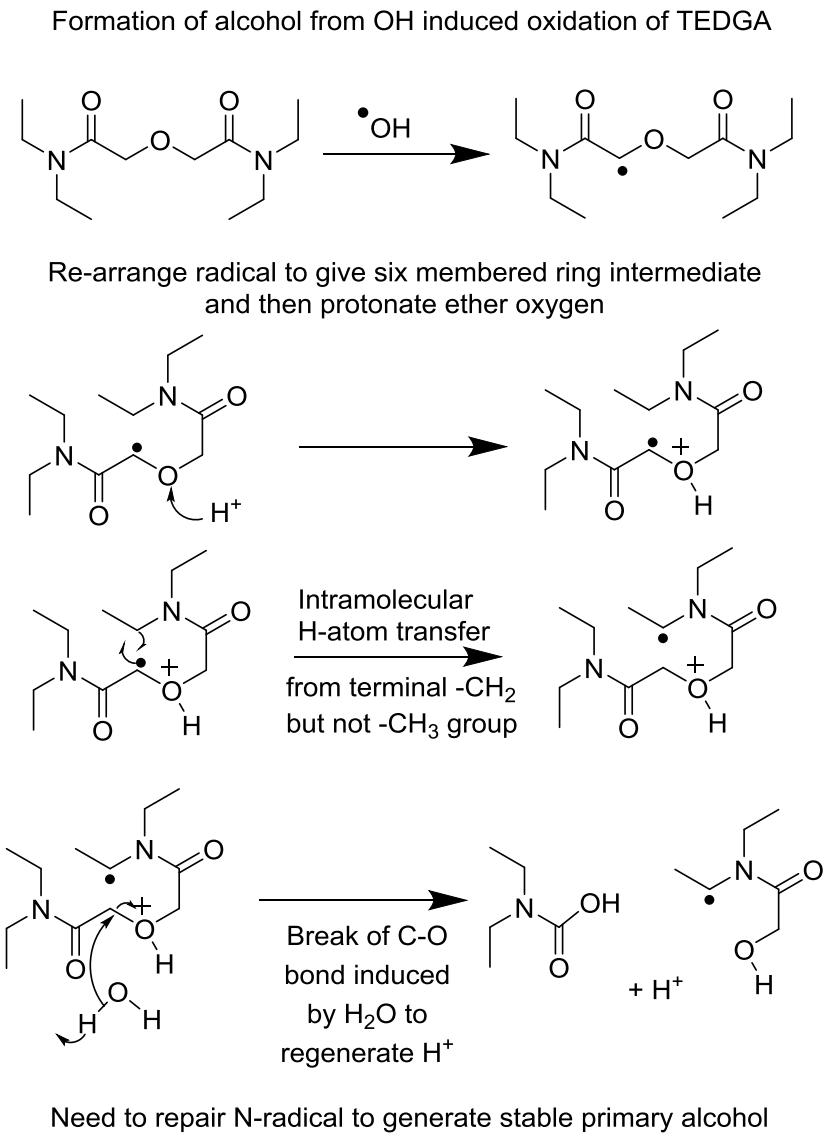

Figure 8. Proposed mechanism for the formation of primary alcohols from $^{\bullet}$OH-induced oxidation of TEDGA.

It should be noted that in practice the hydrophilic DGAs are not used in pure water, rather they are used in nitric acid solution. In solutions concentrated enough to have a significant concentration of undissociated HNO_3, the $^{\bullet}$OH radical is scavenged to produce $^{\bullet}NO_3$ radical. [20] As shown in Table 3, the $^{\bullet}NO_3$ radical reaction decreased by a factor of 5 for TEDGA versus TMDGA. This implies a mechanism other than electron transfer or H-atom abstraction for the reaction of this radical with these DGAs. As was discussed above, the electron transfer reaction rate constants should be similar and fast, while H-atom abstraction rate constants should increase with molecular weight. Addition of the nitrate radical to generate nitrated products is a third possibility. Although such species should be detectable by mass spectrometry, these species were not detected in our study, as all our steady state irradiations/product analyses were conducted in

pure water. However, it must be noted that when lipophilic DGAs in dodecane were irradiated in the presence of aqueous nitric acid, no nitrated products were reported. [7–9]

CONCLUSIONS

The rates of acid degradation and radiolysis of several hydrophilic DGAs were measured. Acid degradation of TEDGA in nitric acid appears to occur by multiple mechanisms, and its rate was significant enough that radiolysis experiments needed to be conducted in pure water. Kinetics measurements revealed fast rate constants for DGA reactions with the $^{\bullet}OH$ radical suggesting that it is an important reactive species involved in the mechanism of DGA radiolytic degradation in water. A decrease in dose constants was found with increasing DGA molecular weight suggesting that predominant mechanism of radical reaction is one of electron transfer rather than H-atom abstraction. Produced DGA radical cations would be expected to be more stable with increasing molecular weight, and thus back reactions would decrease their degradation rate. The radiolysis products identified in aqueous solution are analogous to those previously reported for DGA radiolysis in dodecane, which mechanism was also attributed to electron transfer reactions with the dodecane radical cation.

ACKNOWLEDGEMENTS

Work at INL was funded by the United States Department of Energy (US DOE) Assistant Secretary for Nuclear Energy, Fuel Cycle Research and Development Radiation Chemistry Program, DOE-Idaho Operations Office Contract DE-AC07-05ID14517. Work at CSULB was conducted under US DOE Nuclear Energy Universities program DE-NE-0008406. Financial support for this research was provided by the European Commission from the H2020 Euratom Research and Innovation Programme under grant agreement n°755171 (project GENIORS). We want to thank Beatrix Santiago-Schübel for support with the HRMS measurements.

REFERENCES

1. Mincher, M. E.; Quach, D. L.; Liao, Y. J.; Mincher, B. J.; Wai, C. M. The partitioning of americium and the lanthanides using tetrabutyldiglycolamide (TBDGA) in octanol and ionic liquid solution. *Solvent Extr. Ion Exch.* 2012, 30(7), 735-747. 10.1080/07366299.2012.700583.
2. Sasaki, Y.; Sugo, Y.; Kitatsuji, Y.; Kirishima, A.; Kimura, T.; Choppin, G. R. Complexation and back extraction of various metals by water-soluble diglycolamide. *Anal. Sci.* 2007, 23(6), 727-731. 10.2116/analsci.23.727.
3. Lumetta, G. J.; Gelis, A. V.; Carter, J. C.; Niver, C. M.; Smoot, M. R. The actinide-lanthanide separation concept. *Solvent Extr. Ion Exch.* 2014, 32(4), 333-347. 10.1080/07366299.2014.895638.

4. Rostaing, C.; Poinssot, C.; Warin, D.; Baron, P.; Lorrain, B. Development and validation of the EXAm separation process for single Am recycling. *Procedia Chem.* 2012, 7, 367-373. 10.1016/j.proche.2012.10.057.
5. Lange, S.; Wilden, A.; Modolo, G.; Sadowski, F.; Gerdes, M.; Bosbach, D. Direct selective extraction of trivalent americium from PUREX raffinate using a combination of $CyMe_4BTPhen$ and TEDGA - a feasibility study. *Solvent Extr. Ion Exch.* 2017, 35(3), 161-173. 10.1080/07366299.2017.1326761.
6. Ansari, S. A.; Pathak, P.; Mohapatra, P. K.; Manchanda, V. K. Chemistry of the diglycolamides: Promising extractants for actinide partitioning. *Chem. Rev.* 2012, 112(3), 1751-1772. 10.1021/cr200002f.
7. Zarzana, C. A.; Groenewold, G. S.; Mincher, B. J.; Mezyk, S. P.; Wilden, A.; Schmidt, H.; Modolo, G.; Wishart, J. F.; Cook, A. R. A comparison of the γ -radiolysis of TODGA and T(EH)DGA using UHPLC-MS analysis. *Solvent Extr. Ion Exch.* 2015, 33(5), 431-447. 10.1080/07366299.2015.1012885.
8. Roscioli-Johnson, K. M.; Zarzana, C. A.; Groenewold, G. S.; Mincher, B. J.; Wilden, A.; Schmidt, H.; Modolo, G.; Santiago-Schübel, B. A study of the γ-radiolysis of *N*,*N*-didodecyl-*N'*,*N'*-dioctyldiglycolamide using UHPLC-ESI-MS analysis. *Solvent Extr. Ion Exch.* 2016, 34(5), 439-453. 10.1080/07366299.2016.1212540.
9. Galán, H.; Zarzana, C. A.; Wilden, A.; Núñez, A.; Schmidt, H.; Egberink, R. J. M.; Leoncini, A.; Cobos, J.; Verboom, W.; Modolo, G.; Groenewold, G. S.; Mincher, B. J. Gamma-radiolytic stability of new methylated TODGA derivatives for minor actinide recycling. *Dalton Trans.* 2015, 44(41), 18049-18056. 10.1039/c5dt02484f.
10. Sugo, Y.; Izumi, Y.; Yoshida, Y.; Nishijima, S.; Sasaki, Y.; Kimura, T.; Sekine, T.; Kudo, H. Influence of diluent on radiolysis of amides in organic solution. *Radiat. Phys. Chem.* 2007, 76(5), 794-800. 10.1016/j.radphyschem.2006.05.008.
11. Mezyk, S. P.; Mincher, B. J.; Dhiman, S. B.; Layne, B.; Wishart, J. F. The role of organic solvent radical cations in separations ligand degradation. *J. Radioanal. Nucl. Chem.* 2016, 307(3), 2445-2449. 10.1007/s10967-015-4582-7.
12. Case, M. E.; Fox, R. V.; Baek, D. L.; Mincher, B. J.; Wai, C. M. Extraction behavior of selected rare earth metals from acidic chloride media using tetrabutyl diglycolamide. *Solvent Extr. Ion Exch.* 2017, 35(7), 496-506. 10.1080/07366299.2017.1373984.
13. Mincher, B. J.; Mezyk, S. P.; Elias, G.; Groenewold, G. S.; Riddle, C. L.; Olson, L. G. The radiation chemistry of CMPO: Part 1. *Solvent Extr. Ion Exch.* 2013, 31(7), 715-730. 10.1080/07366299.2013.815491.
14. Mincher, B. J.; Modolo, G.; Mezyk, S. P. Review article: The effects of radiation chemistry on solvent extraction: 1. Conditions in Acidic Solution and a Review of TBP Radiolysis. *Solvent Extr. Ion Exch.* 2009, 27(1), 1-25. 10.1080/07366290802544767.
15. Mincher, B. J.; Mezyk, S. P.; Martin, L. R. A pulse radiolysis investigation of the reactions of tributylphosphate with the radical products of aqueous nitric acid irradiation. *J. Phys. Chem. A* 2008, 112(28), 6275-6280. 10.1021/jp802169v.
16. Buxton, G. V.; Greenstock, C. L.; Helman, W. P.; Ross, A. B. Critical review of rate constants for reactions of hydrated electrons, hydrogen atoms and hydroxyl radicals

(•OH/•O-) in aqueous solution. *J. Phys. Chem. Ref. Data* 1988, 17(2), 513-886. 10.1063/1.555805.

17. Retegan, T.; Berthon, L.; Ekberg, C.; Fermvik, A.; Skarnemark, G.; Zorz, N. Electrospray Ionization Mass Spectrometry Investigation of BTBP - Lanthanide(III) and Actinide(III) Complexes *Solvent Extr. Ion Exch.* 2009, 27(5&6), 663-682. 10.1080/07366290903113991.
18. Fermvik, A.; Berthon, L.; Ekberg, C.; Englund, S.; Retegan, T.; Zorz, N. Radiolysis of solvents containing C5-BTBP: identification of degradation products and their dependence on absorbed dose and dose rate. *Dalton Trans.* 2009,(32), 6421-6430. 10.1039/b907084b.
19. Mincher, B. J.; Modolo, G.; Mezyk, S. P. Review: The Effects of Radiation Chemistry on Solvent Extraction 4: Separation of the Trivalent Actinides and Considerations for Radiation-Resistant Solvent Systems. *Solvent Extr. Ion Exch.* 2010, 28(4), 415 - 436. 10.1080/07366299.2010.485548.
20. Katsumura, Y.; Jiang, P. Y.; Nagaishi, R.; Oishi, T.; Ishigure, K.; Yoshida, Y. Pulse radiolysis study of aqueous nitric acid solutions: formation mechanism, yield, and reactivity of NO_3 radical. *J. Phys. Chem.* 1991, 95(11), 4435-4439. 10.1021/j100164a050.